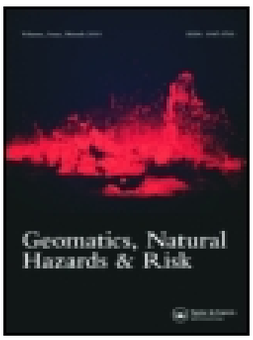

Geomatics, Natural Hazards and Risk

ISSN: 1947-5705 (Print) 1947-5713 (Online) Journal homepage: http://www.tandfonline.com/loi/tgnh20

Landslide quantitative risk analysis of buildings at the municipal scale based on a rainfall triggering scenario

Susana Pereira, Ricardo A. C. Garcia, José Luís Zêzere, Sérgio Cruz Oliveira & Márcio Silva

To cite this article: Susana Pereira, Ricardo A. C. Garcia, José Luís Zêzere, Sérgio Cruz Oliveira & Márcio Silva (2016): Landslide quantitative risk analysis of buildings at the municipal scale based on a rainfall triggering scenario, Geomatics, Natural Hazards and Risk, DOI: 10.1080/19475705.2016.1250116

To link to this article: http://dx.doi.org/10.1080/19475705.2016.1250116

Published online: 04 Nov 2016.

GEOMATICS, NATURAL HAZARDS AND RISK, 2016
http://dx.doi.org/10.1080/19475705.2016.1250116

Taylor & Francis
Taylor & Francis Group

Landslide quantitative risk analysis of buildings at the municipal scale based on a rainfall triggering scenario

Susana Pereira [a], Ricardo A. C. Garcia [a], José Luís Zêzere [a], Sérgio Cruz Oliveira [a] and Márcio Silva [b]

[a]Centre for Geographical Studies, Institute of Geography and Spatial Planning, Universidade de Lisboa, Lisbon, Portugal; [b]Divisão Municipal de Proteção Civil do Porto, Porto, Portugal

ABSTRACT

A landslide quantitative risk analysis is applied the municipality of Santa Marta de Penaguião (N of Portugal) to evaluate the risk to which the buildings are exposed, using a vector data model in GIS.

Two landslide subgroups were considered: landslide subgroup 1 (event inventory of landslides occurred on January 200)1; and landslide subgroup 2 (inventoried landslides occurred after the 2001 event until 2010). Seven landslide predisposing factors were weighted and integrated using the Information Value Method. The landslide susceptibility model was independently validated and the model performance was expressed by ROC curves.

The probability of landslide size was estimated using a probability density function and the landslide hazard scenario was defined using the same landslide rainfall-triggering event.

A vulnerability curve was constructed for each type of building considering its structural properties and the proxy of landslide magnitude. The economic value assigned for each building represents an approximated cadastral value.

The landslide risk was computed for each building in vector format based on a rainfall triggering scenario and two landslide magnitudes.

The probability of occurrence of small landslides is two orders of magnitude higher than the probability of occurrence for large landslides, which explains the higher risk generated by small landslides, despite of registering.

ARTICLE HISTORY
Received 15 July 2016
Accepted 9 October 2016

KEYWORDS
Susceptibility; hazard scenario; vulnerability; landslide risk; shallow slides

1. Introduction

According to Corominas et al. (2013), landslide risk analysis includes the landslide hazard analysis (landslide characterization and analysis of landslide frequency), the analysis of consequences (characterization of expected level of damage for different landslide magnitude scenarios) and risk estimation (the integration of hazard analysis and consequences). Risk assessment takes the output from risk analysis and evaluates risk taking into account values, judgements and risk acceptance criteria. Risk management takes the output from the risk assessment, and considers risk mitigation, including accepting the risk, reducing the likelihood and the consequences (Fell et al. 2008; Corominas et al. 2013).

When risk analysis has to be made for the complete extension of an administrative unit like a municipality and a set of spatial data parameters and the use of GIS techniques are required (Fell & Hartford 1997; Corominas et al. 2013). Landslide risk can be evaluated using qualitative or

CONTACT Susana Pereira susana-pereira@campus.ul.pt

quantitative approaches (AGS 2000; Dai et al. 2002) that are distinguished by the quality and quantity of the input data, analysis procedures, scale of analysis and risk output (Dai et al. 2002; Bell & Glade 2004; van Westen et al. 2008; Corominas et al. 2013). Qualitative risk analysis results are presented in terms of weighted indices and relative ranks (e.g. low, moderate and high) (Corominas et al. 2013). Quantitative risk analysis (QRA) is based on numerical values of the probability, vulnerability and consequences, and the obtained results are presented as a numerical value of the risk (Fell & Hartford 1997; SafeLand 2010) that can be compared with other study areas. Moreover, QRA can include the assessment and quantification of uncertainties (AGS 2000; Corominas et al. 2013). Landslide risk managers benefit from a QRA because it allows a cost–benefit analysis, provides basic information to prioritize management and mitigation actions and the resources allocation (Michael-Leiba et al. 2003; Corominas et al. 2013). Also for society the QRA helps to increase the awareness of existing risk levels and evaluate the effectiveness of actions undertaken (Corominas et al. 2013).

Risk analysis can be done at a national, regional, municipal or local scale. The work-scale should be adequate taking into account the purpose of the assessment, extent of the study area, data availability (Aleotti & Chowdhury 1999), and financial and/or time constraints (Bell & Glade 2004). In addition, some input data layers are only available at a specific scale (van Westen et al. 2008). In such cases, the scale of final results is conditioned by the scale of the input data layer with the lowest resolution. Normally, for small scales QRA is not developed due to the limited quality and quantity of available data. On the contrary, on large-scale studies, there is enough detailed data to perform a QRA (Dai et al. 2002).

Risk is computed as a function of the probability of the landslide hazard (H), the vulnerability (V) and the value of the elements at risk (E) (Varnes 1984): $R = H \times V \times E$, where R is the risk (annual loss of property value); H is the probability of occurrence of a potentially damaging phenomenon within a specified period of time, within a given area and a given magnitude; V is the vulnerability that in earth sciences is usually described as the 'degree of loss' of an element or set of elements at risk resulting from the occurrence of a landslide of given magnitude and it is expressed on a scale ranging from 0 (no loss) to 1 (complete loss) (Varnes 1984; Leóne 1996; Fell & Hartford 1997; Buckle et al. 2000); and E is the economic value of the elements at risk.

Most published studies on landslide QRA in large areas for buildings, roads and properties have been computed using raster data structure (i.e. risk in monetary unit per pixel per year) (e.g. Catani et al. 2005; Remondo et al. 2008; Zêzere et al. 2008; Jaiswal et al. 2011; Garcia 2012; Lu et al. 2013; Peng et al. 2014). Usually, landslide hazard models have been computed in raster data structure where data is stored in grid cells. This data structure enables to handle very large databases and to perform data analysis including mathematical modelling and quantitative analysis (Longley et al. 2011). Raster resolution choice of the initial data used in the landslide susceptibility modelling process can affect the whole analysis and the final results (Arnone et al. 2016). According to Arnone et al. (2016), the best predictive capabilities have been attributed to the medium resolutions (10 and 20 m), proving that the increase in the model resolution does not imply a direct improvement in the model performance.

As a rule, exposed elements data (e.g. roads and buildings) are stored in vector data structure, demanding vector to raster conversion to easily perform risk analysis at the municipal or regional scale. This procedure may generate problems on data integrity due to generalization process linked to the cell size choice taking into account the scale of analysis and the detail of input data. Data conversion of buildings from vector to raster usually produces topological errors (e.g. loss of connectivity between the buildings, creation of false connectivity, loss of individual buildings when their size is smaller than the cell size) and geometrical errors due to the data representation in a regular grid oriented parallel to the coordinate system of the data source (e.g. area, length, geographical position accuracy, changes in the shape and orientation of the buildings) (Longley et al. 2005, 2011).

Most output maps obtained from raster models are not in agreement with high-quality cartographic needs due to the scale of data input (Lee 2004) and the landslide dimensions (Arnone et al.

2016). Also, raster data processing is not suitable for applications that rely on small individual spatial features (points, lines, polygons) (Longley et al. 2005, 2011). Recently, in a study on landslide risk analysis performed for a 169 km^2 study area, Guillard-Gonçalves et al. (2016) estimated a loss of 2.7% of the total area of buildings (which corresponds to 228 buildings in the study case) resulting from the conversion of building features to raster.

On contrary, vector data model guarantees an accurate geographic location of data, accuracy on geometrical properties of buildings, original detail without data generalization and a more aesthetically graphic output (Longley et al. 2005, 2011). To the extent of our knowledge, until now the landslide QRA for buildings represented in a vector data model was never tested at the municipal scale. This type of data model was recently used in a landslide QRA by Uzielli et al. (2014) but only for a reduced number of buildings (39 buildings) within the Ancona landslide.

In this context, the main innovative contribution of this work is to perform a landslide QRA for 7612 single buildings in the municipality of Santa Marta de Penaguião (North of Portugal) in a vector data model within a GIS. In this study area, rainfall is the most important triggering factor of landslides and the relationship between precipitation and landslide activity has been previously studied (Pereira & Zêzere 2012; Zêzere et al. 2015). In order to achieve a landslide QRA, five specific objectives were established: (1) to assess probabilistic landslide hazard based on (a) a susceptibility model for landslide rupture zones, (b) a rainfall-triggering scenario with a specific return period, and (c) the landslide magnitude; (2) to evaluate the physical vulnerability of buildings for different landslide magnitudes based on expert knowledge; (3) to assess the economic value of buildings; (4) to analyse and compare landslide risk at the building scale for two landslide magnitudes ($A_L >$ 100 m^2 and $A_L >$ 1000 m^2).

The landslide susceptibility and hazard were assessed at the local scale, for a complete municipality with and a total area of 70 km^2. The landslide susceptibility was evaluated using a data-driven statistical method that is considered adequate to the regional scale (1:25,000–1:250,000) and the local scale (1:5,000–1:25.000) (Corominas et al., 2013). Results of this study can be used by local stakeholders due to its applicability to the municipal land management.

2. Study area

The municipality of Santa Marta de Penaguião (70 km^2, Figure 1) is located in the Alto Douro Wine Region (Northern Portugal). In geomorphological terms, this area integrates the Portuguese Northwestern mountains (in the west part) and the Douro basin (in the east part) (Ferreira 1991). The elevation ranges from 70 to 1416 m, and the fluvial valleys are deeply incised. The slope angle is higher than 20° in 60.4% of the total area of the municipality.

The study area is part of the Iberian Massif, a morphostructural unit of the Iberian Peninsula which corresponds to the razed Varisc chain (Ferreira 1991). The bedrock includes mostly metamorphic rocks dated from the Cambrian: the Desejosa Formation (fine laminated phyllites, metagreywackes and metaquartzitic greywackes) and the Pinhão Formation (chloritic phyllites, chloritic quartz and metaquartzitic greywackes). Quartzites dated from the Ordovician–Silurian are located in the west part of the study area and syntectonic granites (middle to coarse-grained) are present in the north part of the study area (Figure 1).

The study area has a temperate climate with dry and hot summer, Csa according to Köppen–Geiger climate classification system (Köppen 1936). The mean annual precipitation (MAP) ranges from 700 mm (in the bottom of fluvial valleys in the East side) to 2500 mm (in the Western mountains). Along the year, precipitation is higher during the autumn and winter seasons and the summer drought typically lasts for three months (June, July and August). Rainfall is the main landslide triggering factor in the study area (Zêzere et al. 2015).

Land use is characterized by the predominance of the vineyard monoculture in agricultural terraces (almost 52% of the study area). The remaining area is occupied by forest (16% mainly in the west mountain side of the municipality), pasturelands (13%), degraded forest (8%), discontinuous

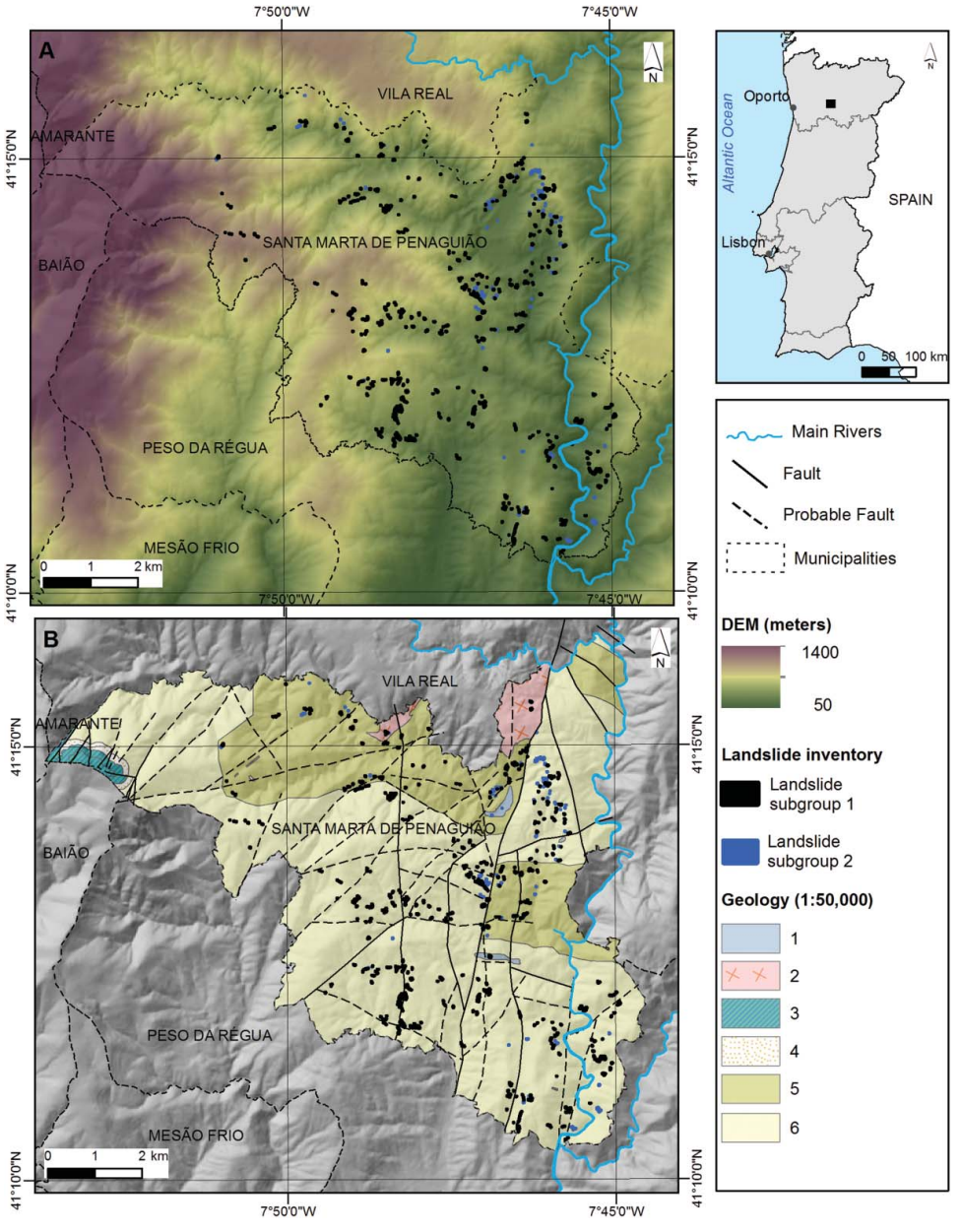

Figure 1. Location of the study area including the distribution of the landslide inventory (*a*) and simplified geological map (*b*) of Santa Marta de Penaguião municipality: (1) alluvium (quaternary); (2) sin-orogenic granite middle- to coarse-grained (carboniferous); (3) quartzites (Ordovician–Silurian); (4) coarse conglomerate (Ordovician–Silurian); (5) Pinhão Formation, with chloritic phyllites, chloritic quartz and metaquartzitic greywackes(Cambrian); (6) Desejosa Formation with fine laminated phyllites, metagreywackes and metaquartzitic greywackes(Cambrian).

urban zones (1%) and other residual land use classes (10%). The viticulture is the major economic activity in the municipality.

Vineyards are mainly located on south-exposed slopes and were traditionally supported by handmade artisanal terrace structures with schist stone and antrosoils. In the last decades, these structures have been replaced by land embankments, without stone support and frequently without efficient drainage systems. Consequently, the slope instability has increased

and several destructive landslides occurred in the study area generating landscape degradation and other human and economic impacts (e.g. deaths and injuries, destruction of houses, and vineyards) (Silva & Pereira 2014).

Historical records of damaging landslides are available in two archive inventories: the North Portugal Landslide Database – NPLD (Pereira et al. 2014) and the Disaster database (Zêzere et al. 2014) with 14 and 1 landslides, respectively.

The municipality had 7356 inhabitants in 2011 (INE 2014) with a population density of 105 inhabitants per km^2. The area is characterized by rural settlements located at the top of the slopes, along the main water divides and on alluvial planes (Silva & Pereira 2014). The typical buildings in the study area are single-story and were built with small blocks of schist. Nowadays, buildings made with bricks and cement are becoming dominant. Residential buildings are the most frequent (63%) followed by farm buildings.

3. Materials and methods

The methodological approach used in this study for the landslide QRA is presented in Figure 2 and involved the following main steps: (1) assessment of the landslide susceptibility rupture zones using a bivariate statistical method (Information Value) and evaluation of model performance based on receiver operating characteristic (ROC) curves; (2) assessment of landslide magnitude based on probability densities of landslide rupture area (Malamud et al. 2004) and using an empirical relationship to link landslide area and landslide volume (Guzzetti et al. 2009); (3) selection of a landslide triggering scenario; (4) estimation of landslide hazard for two landslide magnitudes ($A_L > 100$ m^2 and $A_L > 1000$ m^2); (5) assessment of physical vulnerability of buildings based on empirical vulnerability curves generated for different building types; (6) evaluation of the economic value of buildings and estimation of potential losses; (7) estimation of landslide risk of buildings based on rainfall-triggering scenario referred in (3) and for the landslide magnitudes referred in (4).

3.1. Landslide inventory

A detailed landslide inventory was produced for the municipality of Santa Marta de Penaguião using aerial photo-interpretation (1/5000 scale) of images obtained in 2002, 2005 and 2010, and systematic field work validation (Pereira et al. 2012). The boundaries of the landslide rupture zones were drawn over detailed topographic maps (1/5000 scale) and included in a GIS database.

According to the DISASTER database (Zêzere et al. 2014) for the first time in the last 150 years, fatalities and homeless people were registered on January 2001 following an important landslide event occurred in this municipality previously described by Santos (2013). In fact, most inventoried landslides in the study area occurred during this event, and because of that we decide to consider two subgroups within the landslide inventory: landslide subgroup 1 containing the event inventory of landslides occurred on January 2001, which includes the rupture zones of 610 shallow translational slides with a total unstable area of 94,150 m^2; and landslide subgroup 2 containing all the inventoried landslides occurred in the study area after the 2001 event until 2010, which includes the rupture zones of 156 shallow translational slides with a total unstable area of 10,600 m^2. Shallow translational slides occur in clay-rich metamorphic rocks preferentially located on incised valleys and steep slopes, preferentially south and south-east exposed where agricultural terraces with vineyard dominate.

Data about the landslide area, estimated volume and estimated thickness with the corresponding minimum, maximum, mean, standard deviation and sum values of the landslide subgroups 1 (modelling group) and landslide subgroup 2 (validation group) are summarized in Table 1. Landslide subgroup 1 registered a mean landslide area of 152 m^2 while the landslide subgroup 2 presents

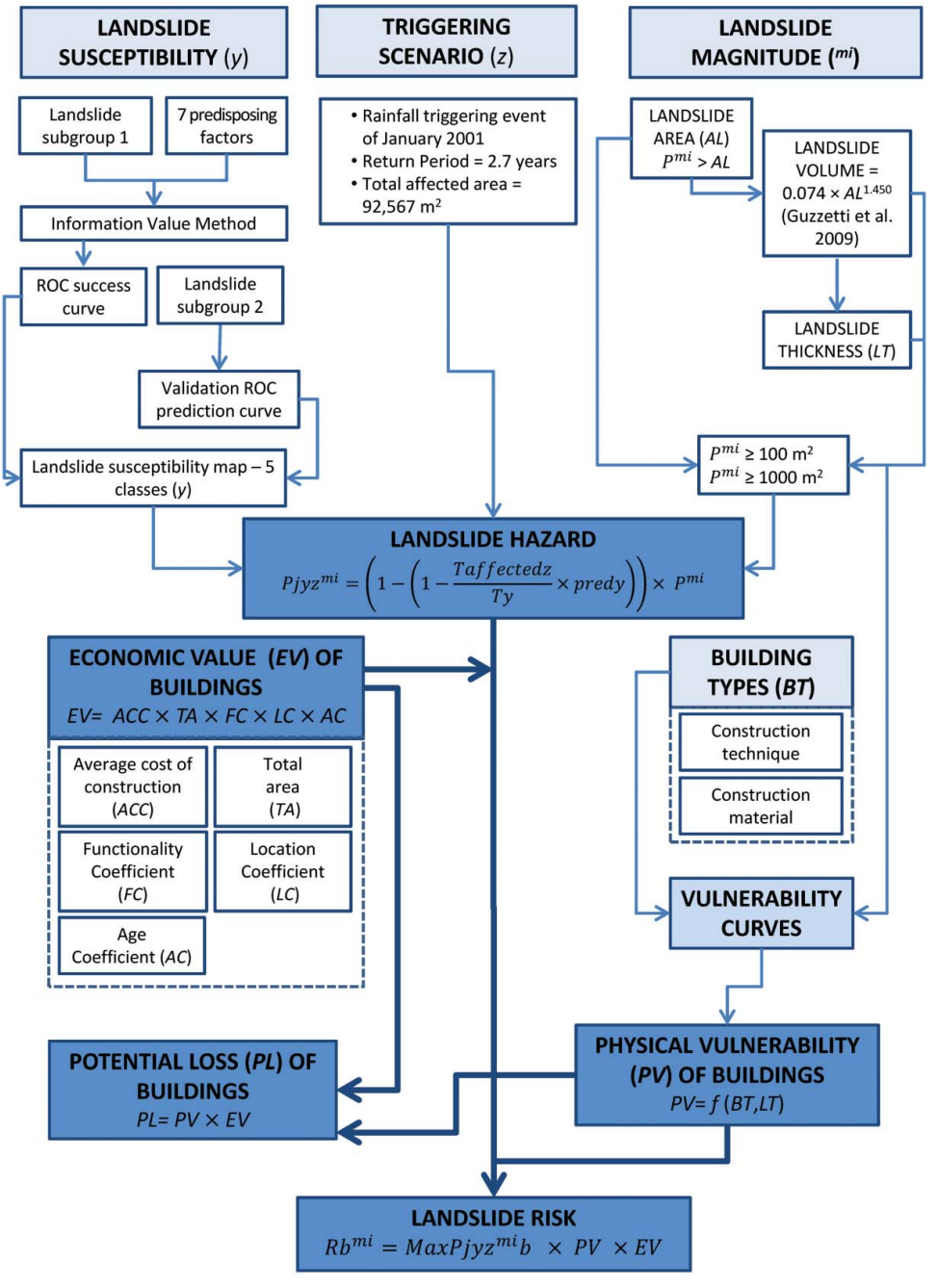

Figure 2. Methodological flowchart of the procedure used.

half of the mean area (71 m^2). As a rule, the size of landslides belonging to subgroup 1 is larger when compared with landslide subgroup 2, as it is confirmed by the corresponding maximum, minimum and mean landslides areas and volumes (Table 1). The total area and total volume of landslide subgroup 1 exceed 9 and 11 times, respectively, the equivalent features of landslide subgroup 2. The landslide thickness, evaluated indirectly based on the relationship between landslide area and

Table 1. Landslide subgroups area, volume and thickness.

		Landslide subgroup 1	Landslide subgroup 2
Number		610	156
Area (m^2)	Minimum	11	5
	Maximum	3141	905
	Mean	152	71
	Standard deviation	232	116
	Sum	94,150	10,600
Estimated	Minimum	2	1
Volume (m^3)	Maximum	8708	1432
	Mean	157	56
	Standard deviation	507	163
	Sum	95,505	8613
Estimated	Minimum	0.2	0.1
Thickness (m)	Maximum	2.8	1.6
	Mean	0.6	0.8
	Standard deviation	0.3	1.4

landslide volume, ranges from a minimum value of 0.1 m in landslide subgroup 1 to a maximum value of 2.8 m in the landslide subgroup 2. The velocity of shallow translational slides can be classified as rapid (1.8 m/h) to very rapid (3 m/min), according to classification proposed by Cruden and Varnes (1996).

3.2. Landslide susceptibility assessment and validation

Landslide susceptibility was modelled using a 10 × 10 m pixel (100 m^2) resolution. The landslide subgroup 1 was used to model susceptibility to landslide rupture zones. This subgroup was cross-tabulated individually with seven landslide predisposing factors used as independent variables (slope angle, slope aspect, slope curvature, slope over area ratio, lithology, geomorphology and land use) that were selected from a list of 29 factors provided by van Westen et al. (2008), which can be relevant as environmental factors effective for landslide susceptibility modelling. The predisposing factors were chosen taking into consideration (1) their high applicability to assess landslide susceptibility at the medium scale (van Westen et al. 2008); (2) the availability of data at the appropriate scale for the study area; (3) the need to minimize conditional independence among predisposing factors to not bias the susceptibility results; and (4) the efficiency of the selected predisposing factors to assess landslide susceptibility confirmed in previous studies in different areas (e.g. Remondo et al. 2003; Zêzere et al. 2004; Guillard and Zêzere 2012) but also in the study area (Pereira et al. 2012). The seven landslide predisposing factors were mapped and converted into a raster format with a 10 × 10 m pixel (100 m^2) and later reclassified for modelling purposes. The classes of each landslide predisposing factor were weighted using the information value method (IV), a bivariate statistical method (Yin & Yan 1988) that has been widely used in similar studies (e.g. Conforti et al. 2011; Guillard & Zêzere 2012; Oliveira et al. 2015), and according to Corominas et al. (2013), this is one of the bivariate statistical methods recommended for data-driven landslide susceptibility assessment.

Information value method weighting of each class within each variable is given as follows (Yin & Yan 1988):

$$\mathrm{IV} = \ln \frac{Si/Ni}{S/N} \tag{1}$$

where Si is the number of pixels with landslides belonging to the modelling group and the presence of variable Xi; Ni is the number of pixels with variable Xi; S is the total number of pixels with

landslides belonging to the modelling group; *N* is the total number of pixels; *Si*/*Ni* is the conditional probability to have a landslide given the presence of variable *Xi*; *S*/*N* is the *a priori* probability for each pixel to have a landslide without considering predisposing factors.

In the present study, the information value scores range from −12,278 to 4277. When the score is negative it means that the presence of the variable is favourable to slope stability. Positive scores mean a positive relationship between the presence of the variable and the landslide occurrence, as high as the higher the score. Information values equal to zero means no clear relationship between the variable and the landslide occurrence. The classes of any variable not containing any landslide have a conditioned probability equal to zero, which means that information value cannot be obtained because of the log transformation, and therefore, the information value was forced to be equal to the decimal value lower than the lowest information value within the variable (Guillard & Zêzere 2012).

Landslide susceptibility map was obtained by the sum of the IV of each variable present in each pixel:

$$\mathrm{IV}j = \sum_{i=1}^{m} Xji \ \mathrm{IV} \tag{2}$$

where *m* is the number of variables and *Xji* is either 0 if the variable is not present in the pixel *j*, or 1 if the variable is present.

Additional details on the predisposing factors applied in Santa Marta de Penaguião municipality can be found in Pereira et al. (2012).

The landslide susceptibility model was validated by cross-tabulation with the landslide subgroups 1 and 2 and the model performance is expressed by ROC curves (Swets 1988). The ROC curve plots the true positive rate (TRP) versus the false positive rate (FPR), where TPR is the proportion of the landslide area that is correctly classified as susceptible and FPR is the proportion of non-landslide area classified as susceptible (Frattini et al. 2010). The area under the ROC curve (AUC) was computed to be a metric of the overall quality of the model (Frattini et al. 2010). An ROC curve was also computed using the landslide subgroup 2, to assess independently the prediction quality of the landslide susceptibility model.

Lastly, landslide susceptibility model computed with the landslide subgroup 1 was classified into five equal-size classes so that the number of cells is the same in each class (20% of the study area), because the respective ROC curve did not show pronounced slope ruptures to identify susceptibility classes.

3.3. Landslide magnitude

An important feature to compute landslide hazard is the landslide event magnitude that may be obtained from landslide inventories, where the size of the landslides (expressed as area or volume) may be used as a proxy of landslide magnitude (Malamud et al. 2004; Guzzetti et al. 2009). Magnitude–frequency curves have been used to obtain a frequency-size distribution and are widely explained in the literature (Malamud et al. 2004; Guthrie & Evans 2004; Guzzetti 2005; Guzzetti et al. 2005; Guzzetti et al. 2008; Brunetti et al. 2009). Once established the relationship between frequency and magnitude of landslides, it is possible to use it to estimate the probability of occurrence of a landslide of certain magnitude (Picarelli et al. 2005). Therefore, the probability density distribution of landslide area (A_L) was computed for the landslides from the landslide subgroups 1 and 2 distribution using the probability density function (pdf) proposed by Malamud et al. (2004). However, the probability of landslide magnitude (A_L) was calculated only for the landslide subgroup 1 to guarantee consistence for the hazard assessment scenario as the landslide susceptibility model was built based on the same landslide subgroup 1.

In addition, landslide area was also used to generate a proxy of landslide intensity that is crucial to estimate the relative level of damages in buildings. In this work the ratio between landslide volume and landslide area was used to estimate landslide thickness of each individual landslide, assuming that shallow translational slides in the study area have a regular shape and thickness.

In the literature, there is a good agreement that the relationship between volume and area of a landslide is essentially geometrical and widely independent on the local physiographical setting (Guzzetti et al. 2009). As determining the volume of a slip is a difficult and expensive task, there are several empirical relationships between landslide area and landslide volume (Guzzetti et al. 2009) that can be applied to different landslide types (e.g. shallow slides and debris flows). Guzzetti et al. (2009) proposed an empirical relationship between landslide area (A_L) and landslide volume (V_L) using 677 landslides compiled through a worldwide literature research, based on landslides with areas ranging between 2.1×10^0 and 7×10^7 m^2 and volumes from 3.4×10^{-1} to 2.9×10^{10} m^3:

$$V_L = 0.074 \times A_L^{1.450} \tag{3}$$

For landslides more similar in size to those inventoried in the study area, Guzzetti et al. (2009) proposed another formula based on data of landslides with areas ranging between 5.0×10^1 and 1.58×10^4 provided by Larsen and Torres-Sánchez (1998):

$$V_L = 1.826 \times A_L^{0.898} \tag{4}$$

However, landslide volumes obtained from equation (4) are not efficient to estimate empirically the landslide thickness as the simple ratio between landslide volume and landslide area. For example, two landslides with 11 and 3141 m^2 (minimum and maximum landslide areas within the landslide inventory) should have 16 and 2523 m^3, respectively, using equation (4). The corresponding landslide thickness derived as the volume/area ration will be 1.4 and 0.8 m, which would indicate lower landslide intensity for the larger landslides. Therefore, we decide to use equation (3) to avoid this drawback. For the same examples, the obtained landslide volumes are 2.4 and 8709 m^3, and the corresponding landslide thickness are 0.2 and 2.8 m. The obtained landslide thickness range is consistent with the field evidences on landslide thickness in the study area.

3.4. Landslide triggering scenario

Most landslides inventoried in the study area (80%) occurred in a single landslide event occurred on 26 January 2001 (Pereira & Zêzere 2012). As the corresponding landslide subgroup (1) was used to generate the landslide susceptibility model, we decided to consider the triggering conditions of this event to define the temporal dimension for the landslide hazard model.

The climatological year of 2000–2001 (the second most rainy since 1960) registered 1914 mm of total annual rainfall (810 mm above the MAP) at the nearest rain gauge (Vila Real). During the winter months of 2000–2001, this rain gauge registered almost the twice of the average rainfall values for the same period (Santos 2013).

Rainfall empirical thresholds of landslides in the study area were assessed in previous works (Pereira 2010; Pereira & Zêzere 2012; Zêzere et al. 2015). Daily rainfall data from a representative rain gauge located at Vila Real was analysed for a 40-year period (1960–2001). During this period, 11 landslide events occurred along the Douro valley were used to compute rainfall empirical thresholds. These landslide events were reconstructed using documental sources (technical scientific documents and newspapers) covering the period 1960–2001. Usually each date is associated to a single reported landslide but newspapers preferentially report only those landslides that generated damaging consequences (Zêzere et al. 2015). As it happens in other studies on rainfall empirical thresholds (Brunetti

et al. 2010; Gariano et al. 2015; Zêzere et al. 2015), landslide events may have been unreported and are probably underrepresented.

For each landslide event, possible rainfall combinations between event rainfall (24–72 h) and antecedent rainfall (5–90 consecutive days) were assessed and the corresponding return periods of the rainfall were calculated using the Gumbel law. The critical rainfall combination with the highest return period is assumed as the critical combination that generated the landslide event.

Therefore, landslide hazard was assessed under the assumption that future occurrence of a rainfall combination (rainfall antecedent + rainfall event) equal to the one verified in 2001, whose return period is 2.7 years, will generate the same consequences regarding slope instability in the study area, i.e. the same number of shallow landslides (610) and equivalent total unstable area (94,150 m^2).

3.5. Landslide hazard quantification

The quantitative hazard assessment at the basin scale has been prior performed in several studies (van Westen et al. 2005; F. Guzzetti et al. 2006; Cascini 2008; Jaiswal et al. 2010; Corominas et al. 2013). In this study, the conditional probability that a pixel will be affected by a shallow translational slide in the future is estimated as follows:

$$Pjyz^{mi} = \left(1 - \left(1 - \frac{T\mathrm{affected}z}{Ty} \times predy\right)\right) \times P^{mi} \tag{5}$$

where $Pjyz^{mi}$ is the probability of the cell j in the landslide susceptibility class y to be affected by a landslide with a specific magnitude ^{mi} within the triggering scenario z, which corresponds in the present study to the January 2001 event that has a 2.7-year return period; $T\mathrm{affected}z$ is the total area to be affected by shallow translational slides within the same triggering scenario z (January 2001 event); Ty is the total area of the landslide susceptibility class y; $predy$ is the prediction capacity of the landslide susceptibility class y; P^{mi} is the probability of landslide magnitude, in the present study $A_L > 100$ m^2 and $A_L > 1000$ m^2.

Equation (5) does not include directly the return period, although this is considered indirectly through the selected triggering scenario z.

3.6. Physical vulnerability assessment of buildings exposed to shallow slides

Physical vulnerability is evaluated as the interaction between the intensity of the hazard and the type of elements at risk (buildings) using vulnerability curves (Corominas et al. 2013). There are several examples of vulnerability studies for different elements at risk computed at pixel units (e.g. Remondo et al. 2008; Zêzere et al. 2008; Jaiswal et al. 2011) and at building features in vector format (e.g. Papathoma & Dominey-Howes 2003; Silva & Pereira 2014; Uzielli et al. 2014).

In this work, the physical vulnerability is assessed for building using semi-quantitative vulnerability curves. Most data needed to identify the building characteristics to assess vulnerability (e.g. construction techniques, construction materials and number of floors) and to assess the economic value of buildings (e.g. average cost of construction, function, location, age) had to be inventoried through a detailed field work. Census data were not used because it only details the statistical subsection (the quarter) and do not provide data for each individual building.

Building cartographic information was vectorized at 1/1000 scale using as cartographic base orthophotomaps from 2006 with 0.5 m resolution (Silva & Pereira 2014). The geographical information was further updated and validated during field work in 2010. At the end, 7612 buildings were vectorized and stored in a GIS database in a vector data model. A photo database was constructed

covering all the inventoried buildings and inquiries were made to the owners of some buildings to clarify any doubt regarding building characteristics (Silva & Pereira 2014).

The physical vulnerability was estimated based on observed damages of past shallow translational slides that affected buildings. Unfortunately, examples of landslide damages in buildings are few in the study area, which does not allow performing a statistical correlation with the degree of damages necessary to derive a validated vulnerability curve.

In the first step, the level of building damage was classified into five discrete classes taking into account published works on the subject (Table 2) (e.g. Alexander 1986; Leóne 1996; AGS 2000; Glade 2003; Tinti et al. 2011; Garcia 2012). Level of damage D0, D1 and D2 do not cause structural damages in the buildings and may require some type of repair. When a building has a level of damage D2 evacuation is needed, although the building structure is not affected. Levels of damage D3 and D4 affect the building structure and evacuation is mandatory. Level of damage D4 implies the immediate need for building demolition. The functionality of the building can be compromised temporarily (D2 and D3) or permanently (D3 and D4). For each average level of damage vulnerability values were assigned, ranging between 0 (no loss) and 1 (total loss) and taking into account previous empirical approaches (e.g. Alexander 1986; Leóne 1996; AGS 2000; Glade 2003; Tinti et al. 2011; Garcia 2012) (Table 2): $V < 0.10$; $V = 0.1$–0.3; $V = 0.3$–0.6; $V = 0.6$–0.8 and $V > 0.8$, for D0, D1, D2, D3 and D4, respectively.

In the second step, the vulnerability was ascribed to four types of buildings (B1 – fragile buildings made with metal or wood; B2 – buildings made with adobe or irregular loose stone walls; B3 – buildings made with bricks or blocks united with cement; B4 – buildings made with reinforced concrete or resistant metal structures) considered by the Portuguese Census (INE 2014) taking into account the landslide thickness, assumed as a proxy of landslide intensity. The obtained vulnerability curves reflect the expert opinion of the authors regarding degree of loss for buildings affected by shallow translational slides but are also based on specialized literature (e.g. (Papathoma-Köhle et al. 2007; Zêzere et al. 2008; Uzielli et al. 2008; Papathoma-Köhle et al. 2012; Guillard-Gonçalves et al. 2016).

In this work, it is assumed that buildings are located in the landslide rupture zone, which means that buildings are subject to dominant horizontal displacements (Glade & Crozier 2005; van Westen et al. 2005; Leóne 2007). Landslides that occur underneath or downslope can cause removal of basal support, collapse, deformation and displacement of the building (Glade & Crozier 2005).

3.7. Economic value assessment for exposed buildings

The monetary value of the buildings can be assessed by calculating a discrete value for each individual building based on (1) cadastral values (e.g. Silva & Pereira 2014) (2) market values (Remondo et al. 2008), and (3) reconstruction costs (e.g. Fuchs et al. 2007; Zêzere et al. 2008; Papathoma-Köhle et al. 2012).

Table 2. Level of building damages generated by landslides and corresponding vulnerability values.

Level of damages	Damages	Vulnerability
D0	Without significant damage: slight accumulation that causes aesthetic degradation.	<0.10
D1	Without structural damages: minor damages that can be easily repaired	0.1–0.3
D2	Without structural damages: important damages with complex reparation (displacement or partial collapse of walls without compromising the structural integrity, severe cracks). Evacuation needed.	0.3–0.6
D3	Structural damages that can affect the stability of the building (displacement or collapse of blocks, partial fall of floors, serious cracks or collapse of structural parts). Immediate evacuation and eventual demolition of the building could be necessary.	0.6–0.8
D4	Damages that seriously compromise the structural integrity of the building (partial or total collapse of the building). Immediate evacuation and demolition.	>0.8

Adapted from Alexander (1989), AGS (2000), Tinti et al. (2011) and Garcia (2012).

Market values and reconstruction costs may be very volatile at the short time and this is the major reason for us to choose the cadastral value to compute the value of the buildings. In addition, adopting this approach the economic value of buildings was objectively quantified using an adaptation of the Portuguese Tax Services equation to determine the taxable value of buildings in Portugal (Silva & Pereira 2014). This equation uses the average cost of construction (AAC), the total area (TA), the functionality coefficient (FC), the location coefficient (LC) and the age coefficient (AC). Additional details on the FC, LC and AC coefficients and on the procedure of economic value calculation for each building can be found in Silva and Pereira (2014).

Potential losses (PL) resulting from landside activity was computed for each single building (polygon features in the GIS) as the product between physical vulnerability (PV) and economic value (EV), expressed in Euros:

$$\mathrm{PL} = \mathrm{PV} \times \mathrm{EV} \tag{6}$$

3.8. Quantitative risk analysis

In order to compute risk values for each building in vector data structure it is mandatory to assign a hazard value for each building. The hazard raster data-set (10 × 10 m cells) was first converted into a vector data model (polygon features) where output polygons were conform to the input raster cell edges. The layer containing the building features was intersected with the hazard layer and for each building polygon a summary was given on the numeric attributes of the polygons in the layer being joined (hazard) based on spatial location. With this operation the maximum and the average hazard probabilities were summarized for each building polygon.

The landslide QRA was computed for each single building in the study area on the basis of the following equation (Guzzetti et al. 1999; Jaiswal et al. 2011; Corominas et al. 2013):

$$Rb^{mi} = \mathrm{Max}Pjyz^{mi}\ b \times \mathrm{PV} \times \mathrm{EV} \tag{7}$$

where Rb^{mi} is the risk for the building polygon for a specific landslide magnitude within the selected triggering scenario z; $\mathrm{Max}Pjyz^{mi}$ is the maximum probability affecting the building area, b; PV is the physical vulnerability of the building, derived from the vulnerability curve that is expressed on a scale ranging from 0 (no loss) to 1(complete loss); and EV is the economic (cadastral) value of the building (in Euros).

The QRA for buildings was assessed for each building in vector data for a specific landslide triggering scenario with a 2.7-year return period including two landslide magnitudes ($A_L > 100$ m^2 and $A_L > 1000$ m^2).

4. Results

4.1. Landslide susceptibility and hazard

The landslide susceptibility model was generated using the 610 shallow translational slides belonging to the landslide subgroup 1 to weighting seven landslide predisposing factors. The ROC curves computed with the landslide subgroups 1 and 2 generated acceptable results (AUC = 0.790 and AUC = 0.776, respectively) according to Guzzetti et al.'s (2006) criteria (Figure 3). The classified results of the landslide susceptibility model are shown in Figure 4. The predictive capacity of landslide susceptibility classes for each landslide subgroup is summarized in Table 3. The landslide susceptibility class 'Very High' occupy 20% of the study area and predict 62% of the landslides belonging to subgroup 1 and 59% of the landslides belonging to subgroup 2.

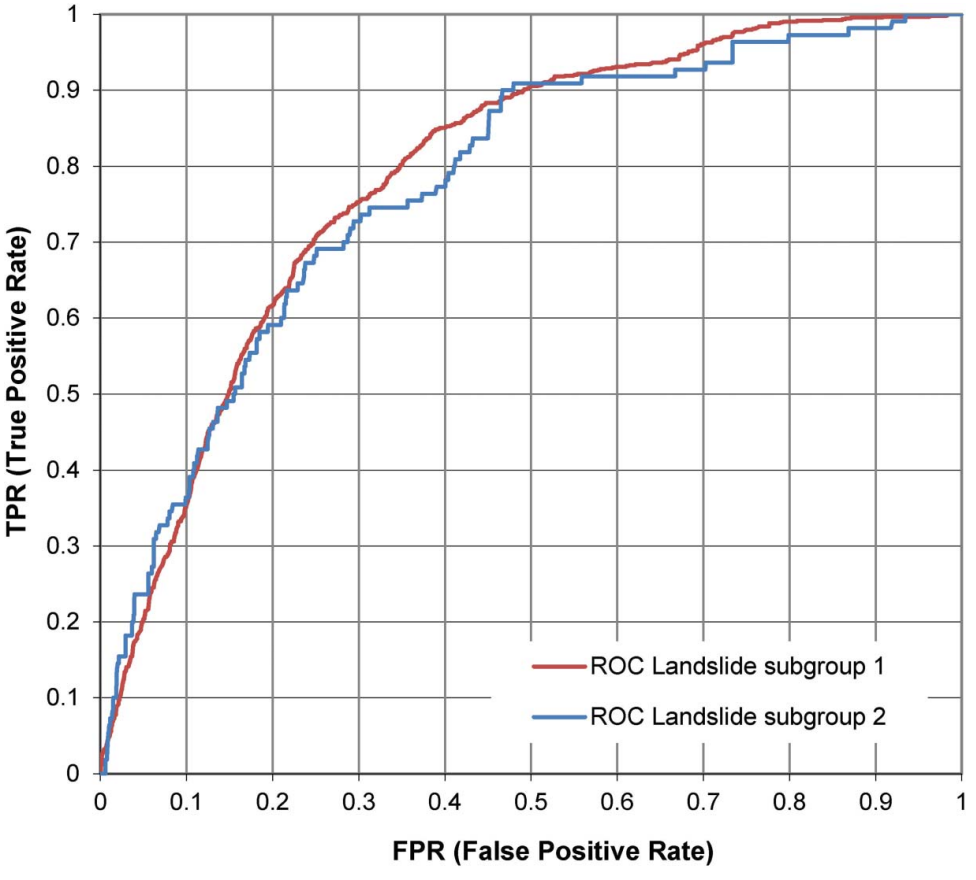

Figure 3. ROC curve of the landslide susceptibility model.

The best result obtained for the January 2001 rainfall-triggered event scenario combines the 72-h event rainfall and the 10-day antecedent rainfall. In previous works (Pereira 2010; Pereira & Zêzere 2012; Zêzere et al. 2015), it was shown that the 26th January 2001 landslide event was triggered by a rainfall event of 97.2 mm in 72 h (return period = 1.7 years) combined with a 10-day antecedent rainfall of 169.9 mm (return period = 1.6 years). The return period of the rainfall combination is 2.7 years considering that the rainfall event and the antecedent rainfall are independent.

The probability density distribution of landslide area (A_L) for the landslide subgroups 1 and 2 is shown in Figure 5(*b*). Landslides more frequent are in the range 10–100 m^2 for landslide subgroup 1 and in the range 5–10 m^2 for landslide subgroup 2, which confirm the typical larger size of landslides belonging to subgroup 1 and explain the absence of any evident roll-over in the landslide subgroup 2. Figure 5(*a*) represents the probability of landslide magnitude having an area smaller than a given size (left axis), and the probability that a landslide will have an area that exceeds a given size (right axis) based on landslide probability density distribution of landslide subgroup 1. The probability that a landslide exceeds an area of 100 and 1000 m^2 is 0.48 and 0.02, respectively. These values were used to obtain the landslide hazard maps for the selected triggering scenario using equation (5). As it was expected, the obtained hazard results expressed as probabilities (Figure 6) are higher for landslides with $A_L > 100$ m^2 (Figure 6(*a*)) than for landslides with $A_L > 1000$ m^2 (Figure 6(*b*)). The maximum hazard per pixel is 0.00171 and 0.00003, for $A_L > 100$ m^2 and $A_L > 1000$ m^2, respectively.

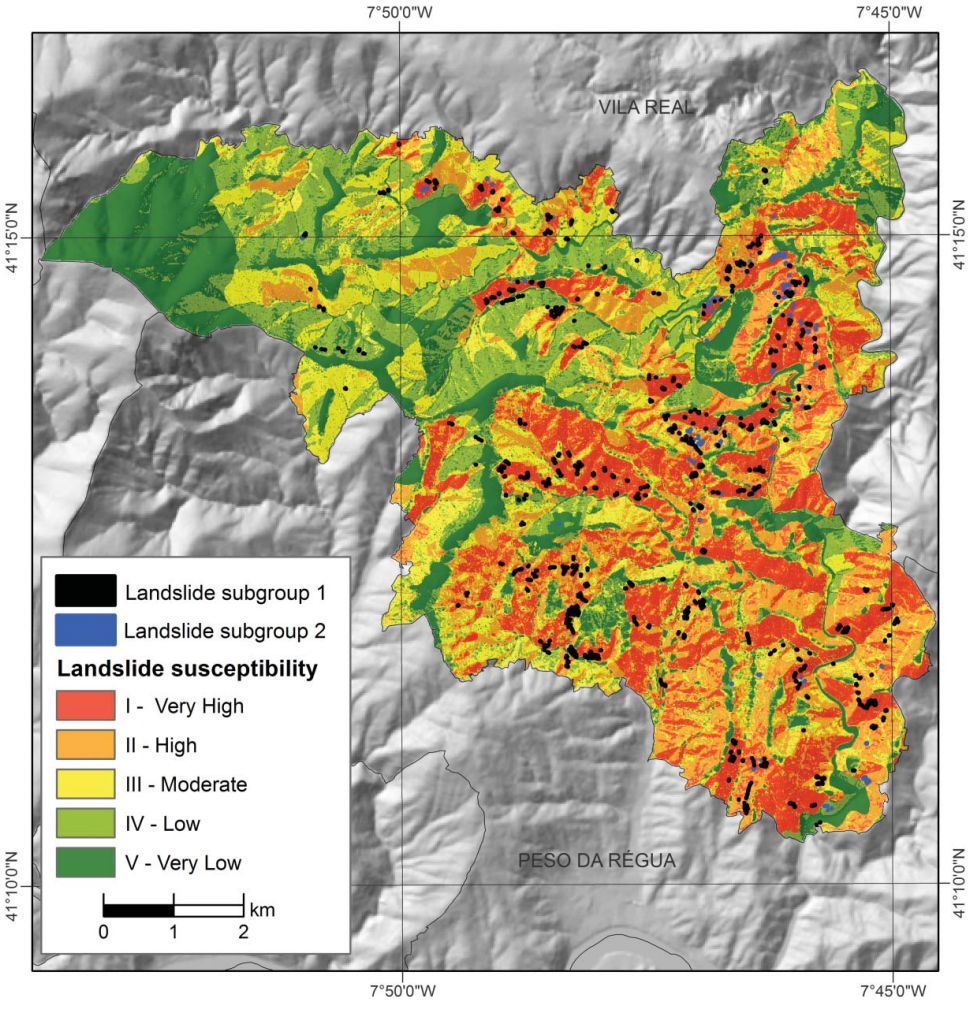

Figure 4. Landslide susceptibility zonation in the Santa Marta de Penaguião municipality.

4.2. Physical vulnerability of buildings

In the study area, more than a half (53.4%) of the 7612 total buildings are type B3 (buildings made with bricks or blocks with cement) whereas 3029 buildings (39.8% of total) are type B4 (buildings made with reinforced concrete or resistant metal structures). Building type B1 (fragile buildings made with metal or wood) and type B2 (buildings made with adobe or irregular loose stone walls) are less in number, corresponding to 6.4% and 0.4% of the total buildings, respectively.

Vulnerability curves generated for each building type (Figure 7) show that shallow slides with 0.5 m thickness cause low level of damages (D2 for building type B1 and D1 for building types B2,

Table 3. Prediction capacity of the landslide susceptibility classes.

Landslide susceptibility class		Class area (%)	Prediction of landslide subgroup 1	Prediction of landslide subgroup 2
I	Very high	20	0.62	0.59
II	High	20	0.23	0.18
III	Moderate	20	0.08	0.15
IV	Low	20	0.06	0.05
V	Very low	20	0.01	0.03

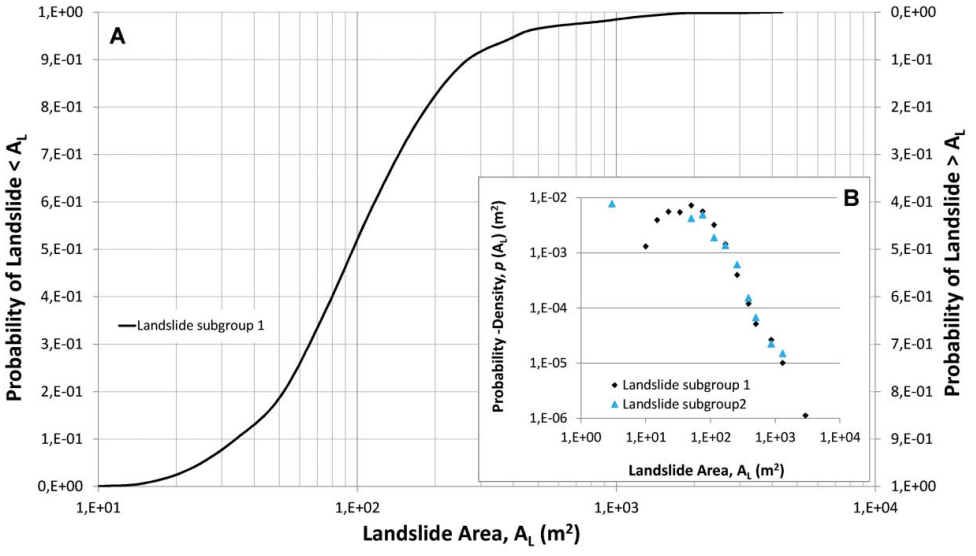

Figure 5. Probability of landslide magnitude (*a*) for landslide subgroup 1 and landslide probability density distribution on landslide area (AL) for landslide subgroup 1 and landslide subgroup 2 (*b*).

B3 and B4) (Table 2). Structural damages (D4) were considered for fragile buildings made with metal or wood (B1) only for landslides with more than 1 m thickness. Buildings made with adobe or irregular loose stone walls (B2) register the highest level of damages (D3) for shallow slides thickness $\geq$ 1.5 m. In the study area, shallow slides do not exceed 2.8 m thickness, so resultant damage in buildings made with bricks or blocks with cement (B3) and buildings made with reinforced concrete or resistant metal structures (B4) do not reach the structural damages (D3 or D4) (Figure 7).

For the landslide magnitude scenario $A_L > 1000$ m^2, the highest values of vulnerability are found for building types B1 and B2, with 1 and 0.8 vulnerability values, respectively (corresponding to level of damages D4 and D3). For the landslide magnitude scenario $A_L > 100$ m^2 (Figure 7), the typical vulnerability of buildings is equal to or less than 0.3 (average level of damages D1), with the solely exception of building type B1 (fragile buildings made with metal or wood) whose vulnerability

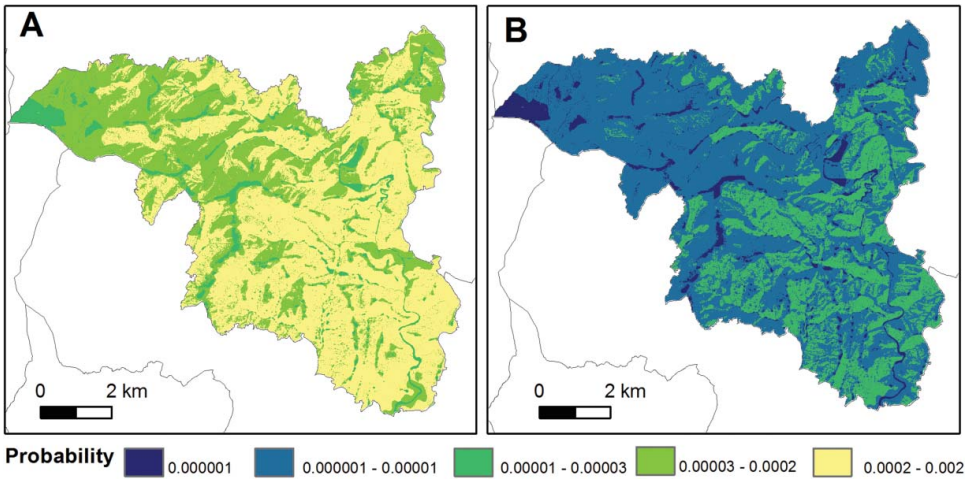

Figure 6. Landslide probability for the landslide magnitude scenarios $A_L > 100$ m^2 (*a*) and $A_L > 1000$ m^2 (*b*) for the considered rainfall-triggering scenario (2.7-year return period).

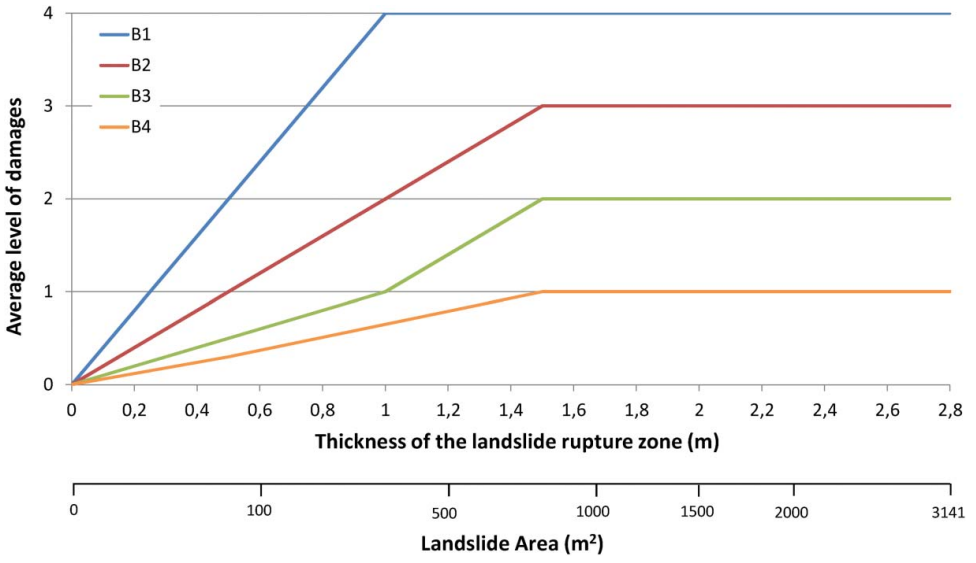

Figure 7. Vulnerability curves according to the building types of the study area. B1 – fragile buildings made with metal or wood; B2 – buildings made with adobe or irregular loose stone walls; B3 – buildings made with bricks or blocks united with cement; B4 buildings made with reinforced concrete or resistant metal structures.

reaches 0.7. In general terms, the residential buildings of the municipality were built with the most resistant materials (B3 and B4). In the worst-case scenario of a shallow landslide with more than 1000 m^2 that hits a B3 or B4 residential building, the average level of damages does not reach structural damages.

4.3. Economic value of buildings

The economic value of buildings in the study area was computed in a previous work (Silva & Pereira 2014). Besides the average cost of construction, economic value of buildings reflects the variation on function, location and age of the building.

Buildings with residential function are dominant in the study area, followed by farm buildings (62.5% and 38.6%, respectively). Buildings with services and commercial functions represent a small percentage (2.5%) and are mainly located in the centre of the municipality.

Figure 8 shows for each building type the correspondent percentage of buildings according to their function. Farm buildings are predominant in more fragile building types, in B1 and B2 (76.7% and 65.8%, respectively). The residential function is dominant in B3 and B4 buildings (54.9% and 78.1%, respectively).

The economic value estimation of each single building is represented in Figure 9(*a*). The economic value of buildings is higher in the village centre (Figure 9(*b*)) and the maximum value corresponds to the building of the Winery Cooperative of Santa Marta de Penaguião (3,870,469 €). On average, buildings with commercial function in the first floor and residential function in the upper floors have the highest economic value (199,962 €), followed by buildings with warehouses and industry (142,831 €) and buildings with residential function (73,998 €). On average, farm buildings have the lowest economic value (4661 €) because typically they are made with fragile wood or metal structures to store farming tools.

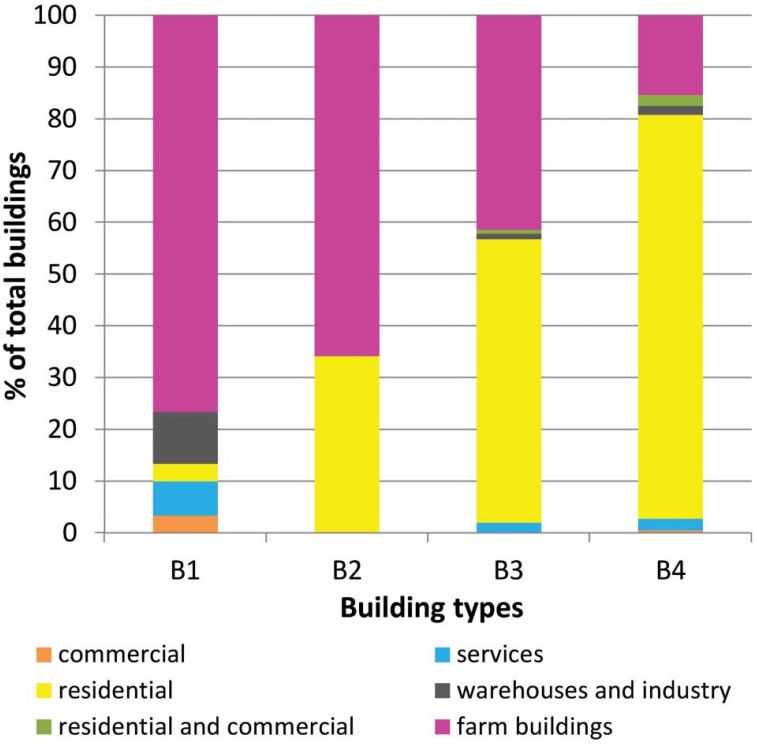

Figure 8. Percentage of uses for each type of building. B1 – fragile buildings made with metal or wood; B2 – buildings made with adobe or irregular loose stone walls; B3 – buildings made with bricks or blocks united with cement; B4 – buildings made with reinforced concrete or resistant metal structures.

4.4. QRA for buildings exposed to shallow slides

The risk (in Euros) for buildings within the municipality of Santa Marta de Penaguião is represented at the building scale for the landslide magnitudes $A_L > 100$ m^2 (Figure 10(*a*)) and $A_L > 1000$ m^2 (Figure 10(*b*)). In both landslide magnitude scenarios, risk classes below 10 euros predominate in the municipality. Also, the number of buildings with very low risk (≤1 €) for landslide magnitude scenario $A_L > 1000$ m^2 is higher than the corresponding feature for landslide magnitude scenario $A_L > 100$ m^2 (93.3% and 39.5% of total buildings, respectively). The maximum value of risk is 1325 € and the average building risk is 8.3 € for the landslide magnitude scenario $A_L > 100$ m^2. On the contrary, the maximum value of risk (38 €) and the average risk per building (0.3 €) corresponding to the landslide magnitude scenario for larger landslides ($A_L > 1000$ m^2) are much lower than equivalent features for the small landslides scenario.

Landslide risk maps for both magnitude scenarios were magnified in the village centre (Figure 11 (*a*,*b*)). Total risk and potential losses associated with each landslide hazard class area are summarized in Tables 4 and 5 for the landslide magnitude scenarios $A_L > 100$ m^2 and $A_L > 1000$ m^2, respectively. Shallow landslide risk values obtained are very low in both scenarios. The potential loss for the scenario $A_L > 1000$ m^2 is near two times higher than the potential loss obtained for the scenario $A_L > 100$ m^2; however, total risk for buildings is 26 times higher for the small landslides scenario ($A_L > 100$ m^2) than for larger landslides scenario ($A_L > 1000$ m^2). The probability of occurrence of small landslides ($A_L > 100$ m^2) is two orders of magnitude higher than the probability of occurrence of large landslides ($A_L > 100$ m^2), which explains the higher risk generated by small landslides, despite the much lower corresponding potential loss.

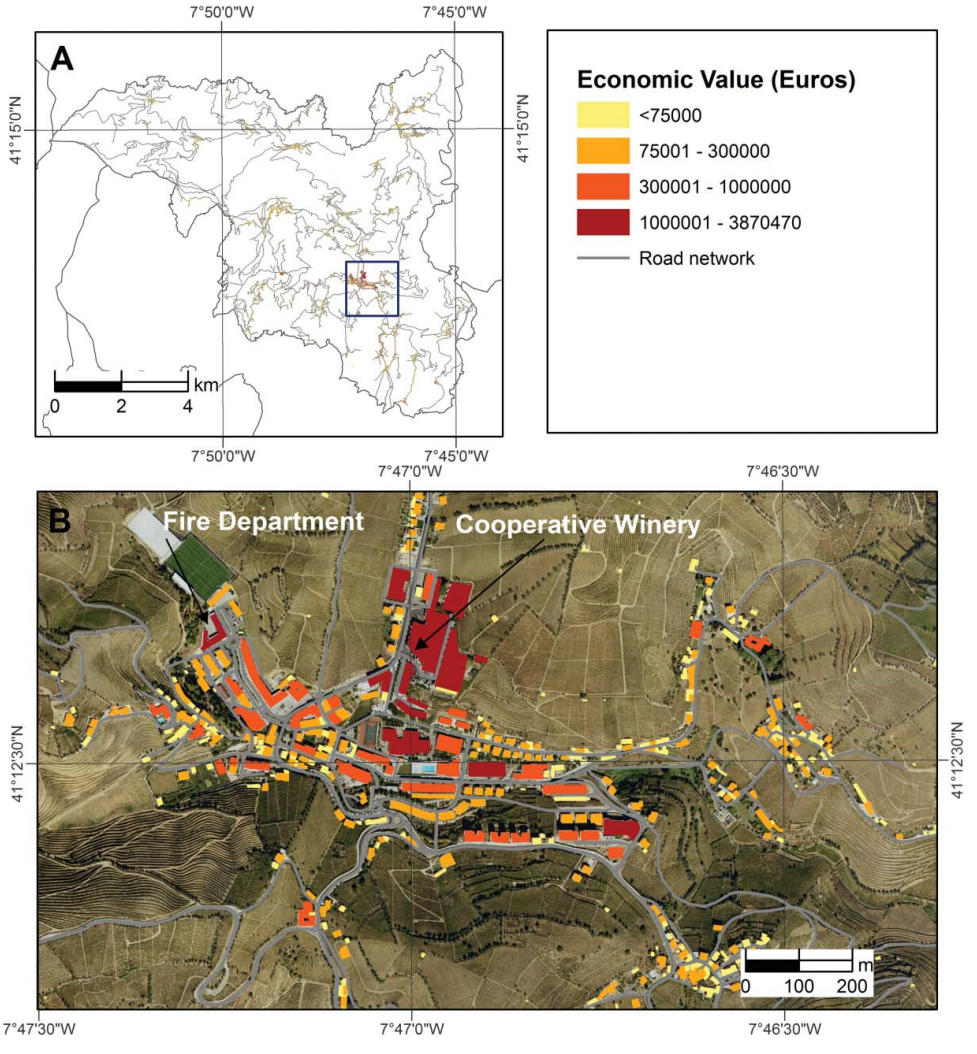

Figure 9. Economic value for the complete set of buildings in the municipality of Santa Marta de Penaguião (*a*) and in the village centre (*b*).

For both magnitude scenarios, it is clear that maximum total risk corresponds to the 'High' landslide hazard class, which contains 20.9% of total buildings within the municipality. On contrary, the 'Very Low' landslide hazard class includes the largest number of buildings (31.2% of total), which explains the highest values of potential losses in both landslide magnitude scenarios.

5. Discussion

The landslide inventory of the study area is certainly not completed but it is based on a well-documented landslide event occurred in 2001 that represents 80% of the total inventory. In addition, uncertainty is also present in the delineation of boundaries of some landslides because of their prompt erase just after the event due to plowing.

Despite the above-mentioned limitations, the landslide area is the most reliable morphometric landslide variable that was systematically collected in landslide inventory for the study area, as it happens in most landslide inventories worldwide (e.g. Galli et al. 2008; Guzzetti et al. 2009).

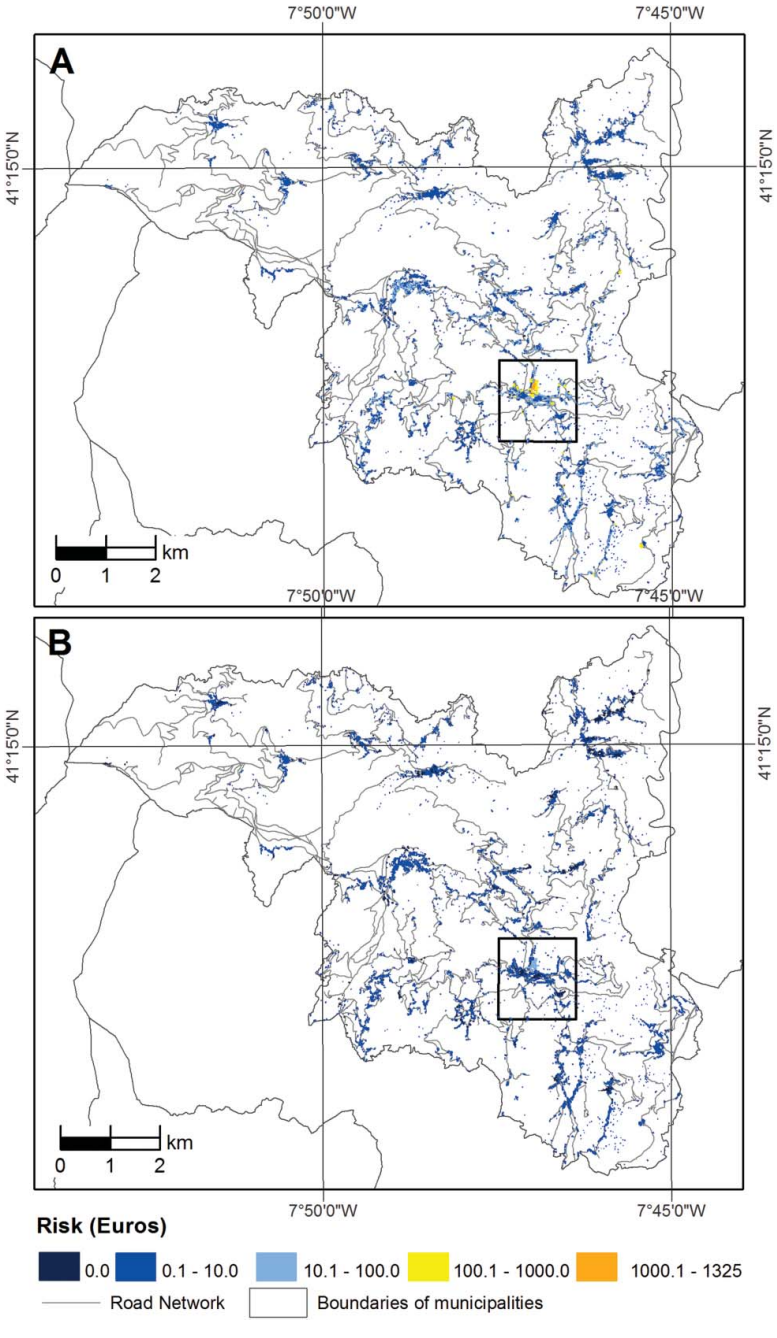

Figure 10. Risk (in Euros) for the complete set of buildings of the municipality of Santa Marta de Penaguião for shallow slide magnitude scenarios of $A_L > 100$ m^2 (a) and $A_L > 1000$ m^2 (b) within the considered rainfall-triggering scenario (2.7-year return period).

In this work, landslide area was used with two purposes: (1) to formalize the complete landslide hazard evaluation using the probability density distribution on landslide area to combine the magnitude probability with the spatial–temporal probability; (2) to use landslide area to derive the landslide thickness using empirical estimations between landslide area–volume–thickness. The landslide thickness is used as a proxy of landslide intensity to construct vulnerability curves for different building types.

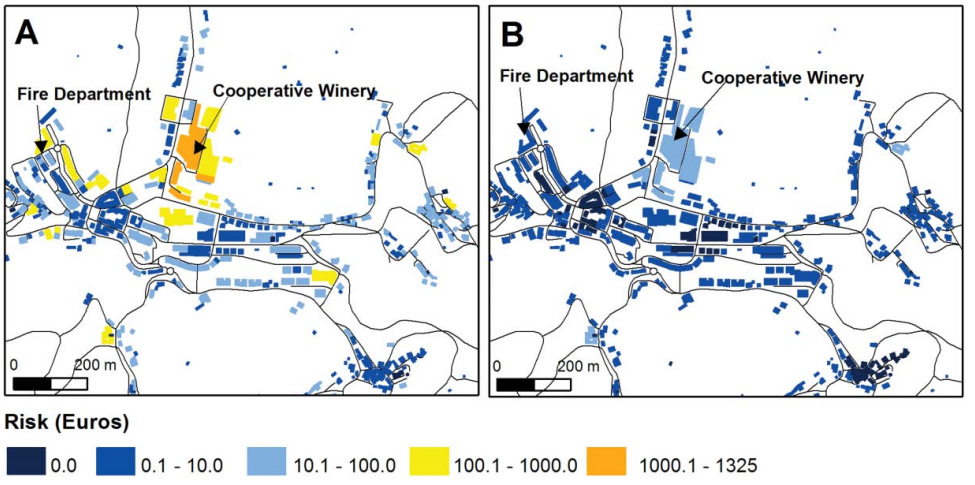

Figure 11. Risk (in Euros) for building located in the village centre of Santa Marta de Penaguião for shallow slide magnitude scenarios of $A_L > 100$ m^2 (*a*) and $A_L > 1000$ m^2 (*b*) within the considered rainfall-triggering scenario (2.7-year return period).

The estimation of landslide thickness as the simple ratio between landslide volume and landslide area is an important source of uncertainty that did not allow adopting a landslide area/volume empirical relationship proposed by Guzzetti et al. (2009) for landslides similar in size to those observed in the study area ($VL = 1.826 \times AL^{0.898}$). On contrary, the adoption of the more general rule proposed by Guzzetti et al. (2009) to relate landslide area and volume ($VL = 0.074 \times AL^{1.450}$) allow to derive realistic landslide thickness for the study area, ranging from 0.2 to 2.8 m, which is in accordance with field work evidence. However, in a recent work, González-Díez et al. (2014) have shown that traditional cartographic methods tend to overestimate landslide volume from 20% to 60%, when compared with digital photogrammetric tools combined with GPS field measurements. Of course, such overestimation will propagate in the next steps of the landslide risk analysis increasing the uncertainty of the final results.

Landslide susceptibility of shallow translational slides was modelled with an event landslide inventory and generated an acceptable ROC curve computed with subgroup 1. In addition, the performance of ROC curve belonging to landslide subgroup 2 is very similar to the ROC landslide subgroup 1, which attests the good prediction capacity of the landslide susceptibility model. The similarity between ROC curves is notable in the area corresponding to the 'Very High' landslide susceptibility class, which validate 59% of total shallow slides occurred after the 2001 event. This is surely not perfect, but quite satisfactory and comparable to results in other similar analyses (Frattini et al. 2010; Pereira et al. 2012).

The temporal dimension of hazard considered the landslide rainfall-triggering event that generated the largest unstable area in the study area in the last 16 years. The January 2001 landslide triggering conditions had an estimated 2.7-return period, combining the 10-day antecedent rainfall and the 72-h event rainfall. Antecedent rainfall is responsible for preparing rock and soil for slope instability

Table 4. Total risk and potential losses associated to the landslide magnitude scenario $A_L > 100$ m^2 for the considered rainfall-triggering scenario (2.7-year return period).

Hazard class	% of buildings	Probability per pixel	Potential loss (€)	Total risk (€)
I – Very high	9.7	1.7×10^{-3}	4,459,760	7634
II – High	20.9	6.5×10^{-4}	13,003,443	17,793
III –Moderate	22.3	2.2×10^{-4}	18,372,477	17,640
IV – Low	16.0	1.6×10^{-4}	15,583,530	9490
V – Very low	31.2	3.0×10^{-5}	32,774,554	10,614
Total	100		84,193,763	63,171

Table 5. Total risk and potential losses associated to the landslide magnitude scenario $A_L > 1000$ m^2 for the considered rainfall-triggering scenario (2.7-year return period).

Hazard class	% of buildings	Probability per pixel	Potential loss (€)	Total risk (€)
I – Very high	9.7	3.3×10^{-5}	9,157,342	297
II – High	20.9	1.3×10^{-5}	26,315,902	597
III – Moderate	22.3	4×10^{-6}	35,490,796	555
IV – Low	16.0	3×10^{-6}	29,527,195	262
V – Very low	31.2	1×10^{-6}	62,201,550	302
Total	100		162,692,786	2013

whereas the event rainfall concentrated in just a few hours is the trigger of landslides (Pereira & Zêzere 2012). This approach allows us to calculate spatial–temporal probabilities for each pixel included in each landslide susceptibility class to be affected by a shallow slide. However, the derivation of rainfall empirical thresholds typically requires many data (e.g. Gariano et al., 2015) that does not exist for the study area. The assumption that future occurrence of an equivalent rainfall combination will generate an equivalent total unstable area is an important source of uncertainty, namely due to the 'event resistance' (Crozier & Preston 1999). However, the relationship between rainfall-event magnitude and landslide density and landslide area is unknown for the study area due to the lack of other past observation. In addition, other rainfall scenarios that were not accounted in this work may generate additional landslide activity in the study area, which means that the annual probability of landslide occurrence is certainly underestimated. Although the 2.7-year return period, the rainfall combination that generated the 2001 landslide event did not repeat from 2001 to 2010, which means that the estimated return period may be underestimated. Moreover, uncertainty regarding the event return period may increase due to changes on frequency of rainfall-triggering events in the study area as a consequence of climate change, which may aggravate the underestimation of landslide probability.

During the period 2001–2010, 156 shallow translational slides occurred in the study area, associated to less severe rainfall conditions, which explain the general lower size of landslides belonging to the subgroup 2 in comparison with landslides of subgroup 1. However, landslides of subgroup 2 are located predominantly in slopes classified as very high and high susceptible to shallow translational slides, which confirms their occurrence under predisposing conditions very similar to those associated to landslide subgroup 1. The considered rainfall-triggering scenario does not allow a QRA for the medium- to long-term, which were not computed for the study area due to the inexistence of landslide inventories associated to other rainfall events with higher return periods.

Physical vulnerability assessment was based on a very detailed field inventory of the buildings characteristics, in contrast to the more usual situation, where information about the buildings is aggregated into statistical units of the census. Physical vulnerability of buildings was assessed for two landslide magnitudes based on expert knowledge. The vulnerability curves represent an estimation of average level of damages that was derived from an empirical relation between the landslide area and the landslide thickness. The number of cases with known landslide thickness is not enough to improve the uncertainty due to the rough evaluation carried out. Moreover, the average level of damage that a landslide of a certain thickness can cause to different types of buildings is another important source of uncertainty, and the proposed vulnerability curves are site specific and should only be applied in areas with similar building characteristics and landslide typology. In addition, vulnerability values correspond to the expected average level of damages in buildings located in the rupture zone of a shallow translational slide where buildings are dominantly affected by horizontal displacement. In this work we did not take into consideration possible damages associated with the landslide propagation. As many shallow slides evolve into debris flows in the study area, the vulnerability values for buildings would be higher, associated with lateral forces and burial.

In this study, it was not possible to validate independently the vulnerability of buildings and the obtained risk assessment. Unfortunately, examples of landslide damages in buildings are few in the study area which did not allowed performing a statistical correlation with the degree of damage necessary to derive a validated vulnerability curve.

The economic value assigned for each building of the municipality represents an approximated cadastral value, not taking into account the supply and demand variation and market speculation, which reflects on both market value and reconstruction cost. The cadastral value of the buildings is the basis used by the Portuguese state to collect taxes on properties and the most reliable value that can be obtained for a complete municipality. Additionally, market values are more volatile and consequently a source of uncertainty higher than the cadastral values of buildings. Also, the value considered does not take into account the building stuff degradation due to landslide activity (Silva & Pereira 2014). People and assets inside the buildings were not considered as well the cost of their temporary relocation. For all these reasons, the economic value of buildings is certainly underestimated.

The risk analysis made at the vector data structure implied to assign to each individual building (independent on its size) a unique value of probability derived from a raster hazard map with 10 m pixel size. In this work, we have chosen the most conservative approach considering the maximum hazard value that is registered inside each building polygon, regardless the area. With this approach, we guarantee that any part of the building have the maximum landslide hazard value considered for the building polygon and consequently the maximum risk value.

Experiences considering the use of the average hazard value, instead of the maximum hazard value would be an acceptable alternative. However, impacts in the landslide risk results should not be neglected for the considered landslide magnitude scenarios. In the present study, the use of a scenario based on the average hazard value would reduce the total risk of buildings in 36% (scenario $A_L > 100$ m^2) and 41% (scenario $A_L > 1000$ m^2).

Risk estimates made for longer periods have greater uncertainties, because it is highly unlikely that the number of exposed buildings, their vulnerability and monetary value will remain unchanged for mid- and long-term. Additionally, long-term risk scenarios should incorporate future changes in the natural system (e.g. precipitation), which is an additional source of uncertainty.

6. Conclusions

Despite the uncertainties related with QRA, the major innovation of this work is the application of a landslide QRA for each single building within a municipality using a vector data model in GIS. The key element of this work is the use of detailed data-sets for each building feature within the municipality in order to quantify potential losses and landslide risk. This methodology enables to maintain the geometrical properties of buildings and to generate a more rigorous quantification of risk. However, this methodology demands a very detailed field survey of the building characteristics at municipal level, which is very time consuming. In practice, this is a constraint to its application to large cities.

Although based on a single rainfall-triggering scenario with a low return period, the proposed QRA allowed a very detailed QRA for buildings exposed to shallow translational landslides applied to a municipality that can be used for the short-term by spatial planning, civil protection and insurance stakeholders. Landslide risk managers benefit from a QRA that provides a strategic tool to the development of cost–benefit analysis, prioritize mitigation actions and emergency resources allocation, and reduce landslide exposure of buildings (Michael-Leiba et al. 2003; Corominas et al. 2013).

Landslides occurred in the study area are triggered by rainfall and although some effort has been made to define rainfall thresholds for landslide initiation(Pereira & Zêzere 2012; Zêzere et al. 2015), the relationship between rainfall events and landslide events magnitude is poorly understood. Of course, the longer the return period, the more severe the rainfall event and hence greater the landslide hazard and risk associated with that return period. However, these relationships are not linear necessarily and cannot be extrapolated from a single event. The development of this line of research will improve the quality of results and will allow the definition of reliable landslide hazard scenarios and QRA for the mid- and long-term.

Acknowledgments

We thank the anonymous reviewers for helpful comments.

Disclosure statement

No potential conflict of interest was reported by the authors.

Funding

S. Pereira and S.C. Oliveira are post-doc fellows of the Portuguese Foundation for Science and Technology (FCT) [grant number SFRH/BPD/69002/2010], [grant number SFRH/BPD/85827/2012]. This work was supported by the project FORLAND – Hydrogeomorphologic risk in Portugal: driving forces and application for land use planning [grant number PTDC/ATPGEO/1660/2014] funded by Fundação para a Ciência e a Tecnologia, Portugal (FCT).

ORCID

Susana Pereira http://orcid.org/0000-0002-9674-0964
Ricardo A. C. Garcia http://orcid.org/0000-0002-1036-6271
José Luís Zêzere http://orcid.org/0000-0002-3953-673X
Sérgio Cruz Oliveira http://orcid.org/0000-0003-0883-8564

References

Australian Geomechanics Society (AGS). 2000. Landslide risk management concepts and guidelines. Aust Geomech Soc Sub-Committee Landslide Risk Manag. :49–92.
Aleotti P, Chowdhury R. 1999. Landslide hazard assessment: summary review and new perspectives. Bull Eng Geol Environ. 58:21–44.
Alexander D. 1986. Landslide damage to buildings. Environ Geol Water Sci. 8:147–151.
Alexander D. 1989. Urban landslides. Prog Phys Geogr. 13:157–191.
Arnone E, Francipane A, Scarbaci A, Puglisi C, Noto LV. 2016. Effect of raster resolution and polygon-conversion algorithm on landslide susceptibility mapping. Environ Model Softw. 84:467–481.
Bell R, Glade T. 2004. Quantitative risk analysis for landslides – Examples from Bíldudalur, NW-Iceland. Nat Hazards Earth Syst Sci. 117–131.
Brunetti MT, Guzzetti F, Rossi M. 2009. Nonlinear Processes in Geophysics Probability distributions of landslide volumes. Nonlinear Process Geophys. 179–188.
Brunetti MT, Peruccacci S, Rossi M, Luciani S, Valigi D, Guzzetti F. 2010. Rainfall thresholds for the possible occurrence of landslides in Italy. Nat Hazards Earth Syst Sci. 10:447–458.
Buckle P, Mars G, Smale S. 2000. New approaches to assessing vulnerability and resilience. Aust J Emerg Manag. 8–14.
Cascini L. 2008. Applicability of landslide susceptibility and hazard zoning at different scales. Eng Geol. 102:164–177.
Catani F, Casagli N, Ermini L, Righini G, Menduni G. 2005. Landslide hazard and risk mapping at catchment scale in the Arno River basin. Landslides. 2:329–342.
Conforti M, Robustelli G, Muto F, Critelli S. 2011. Application and validation of bivariate GIS-based landslide susceptibility assessment for the Vitravo river catchment (Calabria, south Italy). Nat Hazards. 61:127–141.
Corominas J, van Westen C, Frattini P, Cascini L, Malet J-P, Fotopoulou S, Catani F, Van Den Eeckhaut M, Mavrouli O, Agliardi F, et al. 2013. Recommendations for the quantitative analysis of landslide risk. Bull Eng Geol Environ. 73:209–263.
Crozier MJ, Preston NJ. 1999. Modelling changes in terrain resistance as a component of landform evolution in unstable hill country. In: Hergarten S, Neugebauer H, editors. Process Modelling and Landform Evolution. Heidelberg: Springer; p. 267–284.
Cruden DM, Varnes DJ. 1996. Landslide types and processes. In: Turner AK, Schuster RL, editors. Landslides: Investigation and Mitigation. Washington DC: National Academy Press; p. 36–75.
Dai FC, Lee CF, Ngai YY. 2002. Landslide risk assessment and management: an overview. Eng Geol. 64:65–87.
Fell R, Corominas J, Bonnard C, Cascini L, Leroi E, Savage WZ. 2008. Guidelines for landslide susceptibility, hazard and risk zoning for land use planning. Eng Geol. 102:85–98.
Fell R, Hartford D. 1997. Landslide risk management. In: Cruden D, Fell R, editors. Landslide risk assessment – Proceedings of the Workshop on Landslide Risk Assessment. Honolulu, HI: A.A. Balkema; p. 51–119.
Ferreira AB. 1991. Neotectonics in Northern Portugal: a geomorphological approach. Zeitschrift Geomorphol. 82:73–85.
Frattini P, Crosta G, Carrara A. 2010. Techniques for evaluating the performance of landslide susceptibility models. Eng Geol. 111:62–72.
Fuchs S, Heiss K, Hübl J. 2007. Towards an empirical vulnerability function for use in debris flow risk assessment. Nat Hazards Earth Syst Sci. 7:495–506.
Galli M, Ardizzone F, Cardinali M, Guzzetti F, Reichenbach P. 2008. Comparing landslide inventory maps. Geomorphology. 94:268–289.

Garcia RAC. 2012. Metodologias de avaliação de perigosidade e risco associado a movimentos de vertente. Aplicação na bacia da ribeira de Alenquer [PhD in Physical Geography]. Lisbon: Institute of Geography and Spatial Planning, University of Lisbon.
Gariano SL, Brunetti MT, Iovine G, Melillo M, Peruccacci S, Terranova O, Vennari C, Guzzetti F. 2015. Calibration and validation of rainfall thresholds for shallow landslide forecasting in Sicily, southern Italy. Geomorphology. 228:653–665.
Glade T. 2003. Vulnerability assessment in landslide risk analysis. Die Erde. 134:123–146.
Glade T, Crozier MJ. 2005. A review of scale dependency in landslide hazard and risk analysis. In: Glade T, Anderson M, Crozier MJ, editors. Landslide hazard risk. Chichester: John Wiley & Sons, Ltd.; p. 7–138.
González-Díez A, Fernández-Maroto G, Doughty MW, Díaz de Terán JR, Bruschi V, Cardenal J, Pérez JL, Mata E, Delgado J. 2014. Development of a methodological approach for the accurate measurement of slope changes due to landslides, using digital photogrammetry. Landslides. 11:615–628.
Guillard C, Zêzere JL. 2012. Landslide susceptibility assessment and validation in the framework of municipal planning in Portugal: the case of Loures Municipality. Environ Manag. 50:721–35.
Guillard-Gonçalves C, Zêzere JL, Pereira S, Garcia RAC. 2016. Assessment of physical vulnerability of buildings and analysis of landslide risk at the municipal scale – application to the Loures municipality, Portugal. Nat Hazards Earth Syst Sci. 16:311–331.
Guthrie RH, Evans SG. 2004. Analysis of landslide frequencies and characteristics in a natural system, coastal British Columbia. Earth Surf Process Landforms. 29:1321–1339.
Guzzetti F. 2005. Landslide hazard and risk assessment – concepts, methods and tools for the detection and mapping of landslides, for landslides susceptibility zonation and hazard assessment, and for landslide risk evaluation [PhD in Mathematich naturwissenschaftli]. Bonn: Bonn University.
Guzzetti F, Ardizzone F, Cardinali M, Galli M, Reichenbach P, Rossi M. 2008. Distribution of landslides in the Upper Tiber River basin, Central Italy. Geomorphology. 96:105–122.
Guzzetti F, Ardizzone F, Cardinali M, Rossi M, Valigi D. 2009. Landslide volumes and landslide mobilization rates in Umbria, central Italy. Earth Planet Sci Lett. 279:222–229.
Guzzetti F, Carrara A, Cardinali M, Reichenbach P. 1999. Landslide hazard evaluation: a review of current techniques and their application in a multi-scale study, Central Italy. Geomorphology. 31:181–216.
Guzzetti F, Galli M, Reichenbach P, Ardizzone F, Cardinali M. 2006. Landslide hazard assessment in the Collazzone area, Umbria, Central Italy. Nat Hazards Earth Syst Sci. 6:115–131.
Guzzetti F, Reichenbach P, Ardizzone F, Cardinali M, Galli M. 2006. Estimating the quality of landslide susceptibility models. Geomorphology. 81:166–184.
Guzzetti F, Reichenbach P, Cardinali M, Galli M, Ardizzone F. 2005. Probabilistic landslide hazard assessment at the basin scale. Geomorphology. 72:272–299.
[INE] Instituto Nacional de Estatística. 2014. XV Recenseamento Geral da População. Instituto Nacional de Estatística: Lisbon.
Jaiswal P, van Westen CJ, Jetten V. 2010. Quantitative landslide hazard assessment along a transportation corridor in southern India. Eng Geol. 116:236–250.
Jaiswal P, van Westen CJ, Jetten V. 2011. Quantitative estimation of landslide risk from rapid debris slides on natural slopes in the Nilgiri hills, India. Nat Hazards Earth Syst Sci. 11:1723–1743.
Köppen W. 1936. Das geographisca System der Klimate. In: Köppen W, Geiger G, editors. Handbuch der Klimatologie. Gebr: Borntraeger; p. 1–44.
Larsen MC, Torres-Sánchez AJ. 1998. The frequency and distribution of recent landslides in three Montane tropical regions of Puerto Rico. Geomorphology. 24:309–331.
Lee S. 2004. The effect of spatial resolution on the accuracy of landslide susceptibility mapping : a case study in Boun, Korea. Geosci J. 8:51–60.
Leóne F. 1996. Concept de Vulnérabilité Appliqué à l'Évaluationdes Risques Générés par les Phénomènes de Mouvement de Terrain [Thèse de Doctorat de l'Université Joseph Fourier, Grenoble I Sciences, Techniques et Médecine]. Orléans. Editions BRGM.
Leóne F. 2007. Caractérisatión des vulnerabilities aux catastrophes naturelles: contribution à une evaluation géographique multirisque. Montpellier: Universite Paul Valery – Montpellier III. Orléans.
Longley P., Goodchild M, Maguire D, Rhind D, editors. 2005. Geographical information systems: principles, techniques, management and applications. 2nd ed. Chichester: Wiley.
Longley P, Goodchild M, Maguire D, Rhind D. 2011. Geographical Information Systems and Science. 3rd ed. Chichester: Wiley.
Lu P, Catani F, Tofani V, Casagli N. 2013. Quantitative hazard and risk assessment for slow-moving landslides from persistent scatterer interferometry. Landslides. 11:685–696.
Malamud BD, Turcotte DL, Guzzetti F, Reichenbach P. 2004. Landslide inventories and their statistical properties. Earth Surf Process Landforms. 29:687–711.

Michael-Leiba M, Baynes F, Scott G. 2003. Regional Landslide risk to the Cairns community. Nat Hazards. 30: 233–249.
Oliveira SC, Zêzere JL, Catalão J, Nico G. 2015. The contribution of PSInSAR interferometry to landslide hazard in weak rock-dominated areas. Landslides. 12:703–719.
Papathoma M, Dominey-Howes D. 2003. Tsunami vulnerability assessment and its implications for coastal hazard analysis and disaster management planning , Gulf of Corinth, Greece. Nat Hazards Earth Syst Sci. 3:733–747.
Papathoma-Köhle M, Keiler M, Totschnig R, Glade T. 2012. Improvement of vulnerability curves using data from extreme events: debris flow event in South Tyrol. Nat Hazards. 64:2083–2105.
Papathoma-Köhle M, Neuhäuser B, Ratzinger K, Wenzel H, Dominey-Howes D. 2007. Elements at risk as a framework for assessing the vulnerability of communities to landslides. Nat Hazards Earth Syst Sci. 7:765–779.
Peng L, Xu S, Hou J, Peng J. 2014. Quantitative risk analysis for landslides: the case of the three Gorges area, China. Landslides. 12:943–960.
Pereira S. 2010. Perigosidade a movimentos de vertente na Região Norte de Portugal [PhD in Physical Geography]. Oporto: Oporto University.
Pereira S, Zêzere JL. 2012. Empirically-based rainfall thresholds for debris flow occurrence in the North of Portugal. In: González-Diez A (coord), editor. Av la Geomorfol en España 2010-2012 Actas la XII Reun Nac Geomorfol. Santander: Publican Ediciones, Universidad de Cantabria; p. 109–112.
Pereira S, Zêzere JL, Bateira C. 2012. Technical Note: Assessing predictive capacity and conditional independence of landslide predisposing factors for shallow landslide susceptibility models. Nat Hazards Earth Syst Sci. 12:979–988.
Pereira S, Zêzere JL, Quaresma ID, Bateira C. 2014. Landslide incidence in the North of Portugal: Analysis of a historical landslide database based on press releases and technical reports. Geomorphology. 214:514–525.
Picarelli L, Oboni F, Evans SG, Mostyn G, Fell R. 2005. Hazard characterization and quantification. In: Hungr O, Fell R, Couture R, Eberhardt E, editors. Landslide risk management – Proceedings in International Conference on Landslide Risk Management; Vancouver. London: A.A. Balkema; p. 27–71.
Remondo J, Bonachea J, Cendrero A. 2008. Quantitative landslide risk assessment and mapping on the basis of recent occurrences. Geomorphology. 94:496–507.
Remondo J, González A, De Terán JRD, Cendrero A, Fabbri A, Chung C-JF. 2003. Validation of landslide susceptibility maps: examples and applications from a case study in Northern Spain. Nat Hazards. 30:437–449.
SafeLand. 2010. Revision 2. 7th framework programme, Grant Agreement No.: 226479, SGI/ICG revision: 1 – final.
Santos JG. 2013. GIS-based hazard and risk maps of the Douro river basin (north-eastern Portugal). Geomatics Nat Hazards Risk. 6:90–114.
Silva M, Pereira S. 2014. Assessment of physical vulnerability and potential losses of buildings due to shallow slides. Nat Hazards. 72:1029–1050.
Swets JA. 1988. Measuring the accuracy of diagnostic systems. Science 240:1285–1293.
Tinti S, Tonini R, Bressan L, Armigliato A, Gardi A, Guillande R, Valencia N, Scheer S. 2011. Handbook of tsunami hazard and damage scenarios. SCHEMA, Scenarios for Hazard-Induced Emergency Management. JRC Scientific and Technical Reports. Luxembourg: Publications Office of the European Union.
Uzielli M, Catani F, Tofani V, Casagli N. 2014. Risk analysis for the Ancona landslide – II: estimation of risk to buildings. Landslides. 12:83–100.
Uzielli M, Nadim F, Lacasse S, Kaynia AM. 2008. A conceptual framework for quantitative estimation of physical vulnerability to landslides. Eng Geol. 102:251–256.
van Westen CJ, van Asch TWJ, Soeters R. 2005. Landslide hazard and risk zonation – why is it still so difficult? Bull Eng Geol Environ. 65:167–184.
van Westen CJ, Castellanos E, Kuriakose SL. 2008. Spatial data for landslide susceptibility, hazard, and vulnerability assessment: an overview. Eng Geol. 102:112–131.
Varnes D., International Association of Engineering Geology Commission on Landslides and Other Mass Movements on Slopes. 1984. Landslide hazard zonation: a review of principles and practice. Paris: UNESCO.
Yin KL, Yan TZ. 1988. Statistical prediction models for slope instability of metamorphosed rocks. In: Bonnard C, editor. Proceedings of Fifth International Symposium on Landslides. Rotterdam: Balkema; p. 1269–1272.
Zêzere JL, Garcia Ra.C, Oliveira SC, Reis E. 2008. Probabilistic landslide risk analysis considering direct costs in the area north of Lisbon (Portugal). Geomorphology. 94:467–495.
Zêzere JL, Pereira S, Tavares AO, Bateira C, Trigo RM, Quaresma I, Santos PP, Santos M, Verde J. 2014. DISASTER: a GIS database on hydro-geomorphologic disasters in Portugal. Nat Hazards. 72:503–532.
Zêzere JL, Reis E, Garcia RAC, Oliveira SC, Rodrigues ML, Vieira G, Ferreira AB. 2004. Integration of spatial and temporal data for the definition of different landslide hazard scenarios in the area north of Lisbon (Portugal). Nat Hazards Earth Syst Sci. 4:133–146.
Zêzere JL, Vaz T, Pereira S, Oliveira SC, Marques R, Garcia RAC. 2015. Rainfall thresholds for landslide activity in Portugal: a state of the art. Environ Earth Sci. 73:2917–2936.